Investigation of Electrical Properties of CIGS/n-Si Heterojunction Solar Cell in Darkness and Light Environments

Serap YİĞİT GEZGİN[1], Yasemin GÜNDOĞDU[2] and Hamdi Şükür KILIÇ[1,3,4]

***Abstract*—** We have produced an Ag/CIGS/n-Si/Al heterojunction solar cell for this study. CIGS ultrathin film grown by PLD system have been examined in terms of the morphology, crystalline and optical properties. The crystalline size of CIGS ultrathin film, which has a single crystal structure, has been calculated by Scherrer equation. Micro strain and dislocation density of CIGS ultrathin films have been determined. Indium-rich CIGS ultrathin film's stoichiometric transfer was deviated by a little. J-V curves of CIGS/n-Si solar cell and its electrical properties have been investigated as well as determined for the darkness and illumination environments. The ideality factor, serial resistance and barrier height of the solar cell were calculated using the conventional J-V, Norde and Cheung-Cheung methods. The electrical parameters of CIGS solar cells have also been investigated for both environments and the results have been discussed in this study.

***Keywords*—**CIGS ultrathin film, PLD, solar cell, heterojunction,

I. Introduction

CIGSe material is used to be an active layer in solar cells, being dominant in the thin-film photovoltaic (PV) market. $Cu_2In_{(1-x)}Ga_xSe$ has a high absorption coefficient, adjustable band gap depending on the *x* value and high chemical and physical stabilities [1, 2]. CIGS material is often applied in thin-film solar cells to be a p-type semiconductor in the production of p-n heterojunction solar cells based Silicon (Si) for tandem solar cells [3, 4]. The limited efficiency of thin-film solar cells has led PV world to produce tandem solar cells. The experimental as well as many theoretical studies has being performed on the tandem solar cell. In the last few years, as a preliminary study for the production of CIGS tandem solar cells, efficiency improvement studies have been carried out in p-CIGS/n-Si heterojunction solar cells [5]. The fact that Si wafer is cheap and environmental friendly and has no impurity in its structure, and these properties gives it a great advantageous for tandem solar cells [3, 4].

PLD technique is a very powerful technique for the production of complex structured materials which composed of four-elements such as CIGS. PLD has adjustable parameters such as substrate temperature, laser fluency, back ground gas pressure and laser wavelength for thin film production with desired properties. Especially, stoichiometric transfer, crystalline and epitaxial growth in low substrate temperature and low material consumption by PLD technique are all very important factors which are sought in the production of the solar cells [5].

In this study, we have grown CIGS ultrathin film on n-Si wafer by PLD and then fabricated Ag/CIGS/n-Si/Al heterojunction solar cell by depositing Ag and Al front and rear contacts with Physical Vapour Deposition (PVD) system. Scanning Electron Microscopy (SEM), UV-vis spectroscopy, X-Ray Diffraction (XRD) methods were used to examine CIGS ultrathin film's morphological, optical and crystalline properties. In both dark and illumination environments, J-V characteristics of CIGS/n-Si heterojunction solar cells were obtained. The electrical parameters of the heterojunctions were calculated and compared using the conventional, Norde and Cheung-Cheung methods. In addition, PV parameters have been determined.

II. Experimental

In this study, before the experiment process started, we have cleaned the soda lime glass (SLG) and Si wafer in the necessary procedure, as we explained in our previous study [6]. PVD technique was used to deposit Al contact in 100 nm thickness on Si wafer's back surface. In the PLD system, before start experimenting, the distance between target material on which materials ablated by laser and substrate on which ablated materials deposited was set at 45 mm. The vacuum chamber was evacuated down to a background pressure of to ~10^{-6} mbar. A laser beam (with 35 mJ energy, 1064 nm wavelength and a 10 Hz repetition rate) has been applied to ablate materials from CIGS sputtering target (% 99.99 pure) and then CIGS ultrathin film has been deposited on n-Si wafer front surface and SLG at room temperature by

Serap YİĞİT GEZGİN, [1]Department of Physics, Faculty of Science, University of Selcuk, Turkey

Yasemin GÜNDOĞDU, [2]Department of Electric and Energy, Kadınhanı Faik İçil Vocational High School, University of Selçuk, Turkey.

Hamdi Şükür KILIÇ, [1]Department of Physics,Faculty of Science, University of Selcuk, [3]Directorate of High Technology Research and Application Center, University of Selcuk, [5]Directorate of Laser Induced Proton Therapy Application and Research Center, University of Selçuk Turkey.

https://doi.org/10.17758/EIRAI10.F1021110

28000 laser pulse number. Both CIGS ultrathin films were annealed for 30 minutes at 450°C temperature in the quarts tube furnace. Then, PVD technology was used to deposit Ag contact in 100 nm thickness on CIGS ultrathin film, resulting in Ag/CIGS/n-Si/Al solar cell shown in Fig.1.

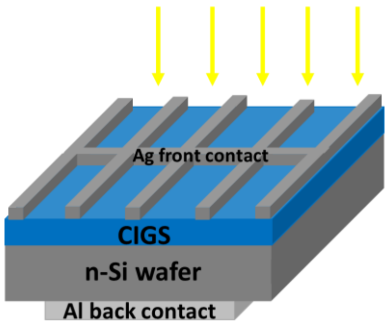

Fig. 1. The diagram image of Ag/CIGS/n-Si/Al heterojunction solar cell

III. Discussion

A. The Crystalline, Morphologic And Optical Characteritics Of Cigs Ultrathin Film

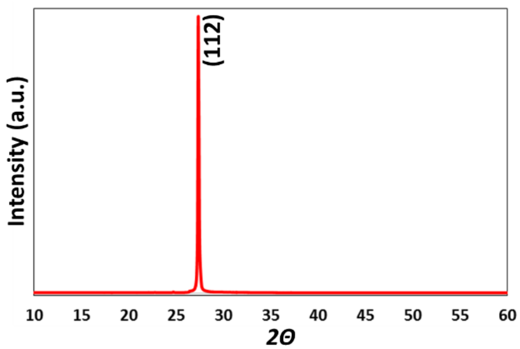

Fig. 2 XRD pattern of CIGS ultrathin film

It has been found that CIGS ultrathin film produced in 420 nm thickness has a dense main peak in (112) orientation on $2\theta=27.34^{o}$ [7-9], according to XRD pattern given in Fig. 2. The crystalline size of CIGS ultrathin film in the single crystal was calculated by applying Scherrer equation:

$$D = 0.94\lambda/\beta cos\theta \tag{1}$$

where D is crystalline size, β is the full-width at half-maximum of diffraction peak, λ is wavelength of X-Ray and θ is Bragg diffraction angle. CIGS ultrathin film has high main crystalline size of 65.71 nm, according to calculations.

The dislocation density (δ) and microstrain (ε) of thin films, which refers to defect formations that adversely affect the crystal structure of thin films [10, 11], can be calculated by Eq.(2) and Eq.(3),

$$\delta = 1/D^2 \tag{2}$$

$$\varepsilon = \beta cos\theta/4 \tag{3}$$

The dislocation density and micro-strain values of CIGS ultrathin film have been determined to be 0.2×10^{15}(lines/m^2) and 0.55×10^{-3}. Since δ and ε values are small, CIGS ultrathin film's crystalline structure is developed.

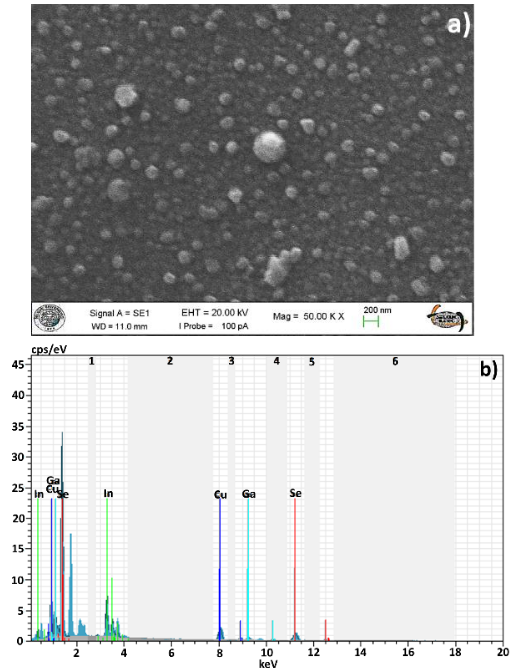

Fig. 3 a) SEM image and **b)** EDX Spectrum of CIGS ultrathin film

TABLE I

THE ELEMENT RATES IN CIGS ULTRATHIN FILMS

Thin film	*Cu(%)*	*In(%)*	*Ga(%)*	*Se(%)*	*Cu/In+Ga*	*S/metal*
CIGS	28.73	22.67	5.50	43.10	1.01	0.75

CIGS ultrathin film consists particles in heterogeneous size distribution and in sizes larger than 150 nm, as seen in SEM image in Fig. 3a. CIGS thin film is In rich due to EDX spectrum in Fig. 3b and the data given in Table 1. Cu and (In+Ga) ratios are very close to each other. The ratio of Se to metal is less than 1 and there is slightly deviation from the stoichiometric transfer.

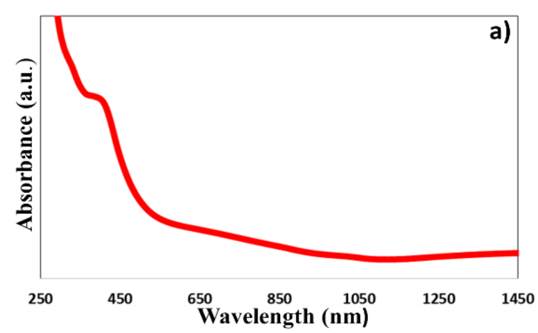

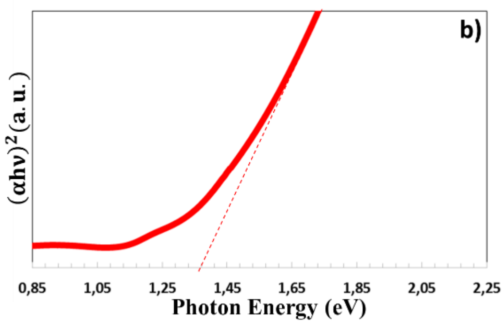

Fig. 4 a) Absorbance spectrum and **b)** Tauc graph of CIGS ultrathin film

CIGS ultrathin film tends to absorb light from the visible region to UV region and has an absorption peak in the 400-450 nm range, in the absorption spectrum given in Fig. 4a. The Tauc equation, which is given below, was used to calculate the band gap of the thin film:

$$(\alpha hv)^2 = A\left(hv - E_g\right)^{1/2} \tag{4}$$

where hv is the energy of photon, A is a constant and E_g is thin film band gap. The straight line of $(\alpha hv)^2$ versus (hv) in Tauc plot in Fig. 4b determines E_g band gap of CIGS thin film. According to this, CIGS ultrathin film's E_g value was calculated to be 1.37 eV and consistent with the values found in the literature [12].

B. Electrical Properties Of CIGS/N-Si Heterojunction Solar Cell In The Darkness And Illumination

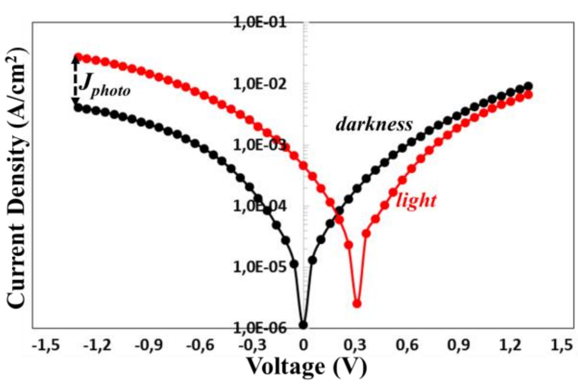

Fig. 5 The logarithmic (log) *J-V* curves of CIGS/n-Si heterojunction solar cell in the darkness and illumination

The rectification rates (*RR*) are expressed by the ratio of forward current at +1V to reverse current at -1V, which of CIGS heterojunction in the dark and illumination were found to be 2.22 and 0.24, respectively, according to log J-V curve in Fig.5. *RR* values of CIGS hetero-junctions was measured to bb very small for illumination conditions because the photocurrent in the reverse bias increases due to the formation of photo-excited charge carriers [13, 14].

The photocurrent density (J_{photo}) can be estimated by the equation stated below:

$$J_{photo} = J_{illumination} - J_{dark} \tag{5}$$

where, $J_{illumination}$ is the current in reverse bias region for illumination, J_{dark} is the current in reverse bias region for darkness environment [15]. J_{photo} of CIGS/n-Si heterojunction solar cell has been calculated to be 0.022 A/cm^2.

A diode's current and ideality factor [16, 17] has been given by Eq. (6) and (7), according to thermionic emission theory:

$$I = I_0[exp(qV/nkT) - 1] \tag{6}$$

$$n = \frac{q}{kT}\frac{dV}{d(lnI)} \tag{7}$$

where I_o, V, k, n, q and T are the saturation current, the forward bias voltage applied, Boltzman constant, the ideality factor, electric charge and the absolute temperature, respectively. A direct line is drawn in forward bias of log (J-V) to determine the ideality factor. *n* values of CIGS heterojunction for the darkness and illumination conditions was determined to be 2.90 and 3.71 in Table II, respectively. The higher ideality factor for the illumination can be attributed to that photo-excited charge carriers cause undesired charge transfer in the interfacial region of the depletion region.

Eq. (8) is used to determine a diode's barrier height (ϕ_b):

$$\phi_b = \frac{kT}{q} ln\left(\frac{AA^*T^2}{I_0}\right) \tag{8}$$

where A and A^* are the active area of diode and Richardson constant (112 A cm^{-2}K^{-2} for n-Si), respectively. I_o is identified by a straight line drawn intersects with y-axis of the reverse bias in the log (J-V) curve in Fig. 5. The barrier heights determined for dark and illumination conditions were found as 0.54 eV and 0.49 eV, respectively [18, 19]. The lower ϕ_b value for illumination condition can be explained due to electric field formed by photo-excited charge carriers in the illumination [20]. In addition, to the illumination environment, a higher saturation current can result in a low barrier height.

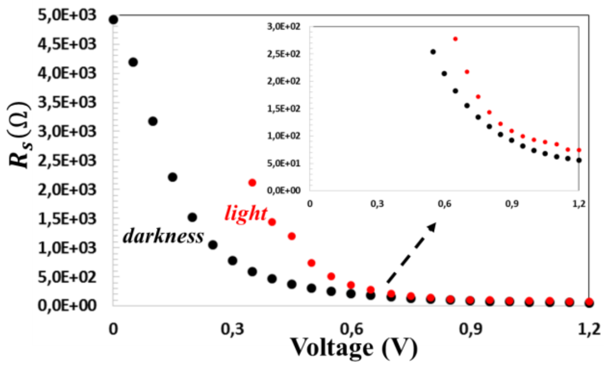

Fig. 6. R_s-V curves of CIGS/n-Si heterojunction solar cell in the darkness and illumination

The serial (R_s) resistance [21] of the hetero-junction can be calculated using eq. (9):

$$R_s = \frac{\Delta V_{forward\ bias\ voltage}}{\Delta I_{forward\ bias\ current}} \quad (9)$$

Serial resistance is an important parameter that affect the efficiency of the solar cell and calculated by the ratio of the voltage difference to the current difference in forward region. From R_s-V curve drawn in Fig. 6 using Eq. (9), R_s values of CIGS heterojunction in the darkness and illumination conditions have been calculated to be 54.63 Ω and 66.33 Ω, respectively. The series resistance values for both environments have been found to be close to each other. Contact resistances, interface defects, pinhole formations in CIGS ultrathin film can cause the serial resistance of the solar cell [6].

TABLE II

THE ELECTRICAL PARAMETERS CALCULATED USING THE CONVENTIONAL J-V, CHEUNG CHEUNG AND NORDE METHODS TO THE DARKNESS AND ILLUMINATION

Parameters			***Dark.***	***Illumin.***
The Conventional	***J-V***	***n***	2.90	3.71
		ϕ_b (eV)	0.54	0.49
		R_s (Ω)	54.63	66.33
Cheung Cheung	***dV/dln(J)***	***n***	6.57	3.86
		R_s (Ω)	32.72	52.00
	H(J)	***ϕ_b (eV)***	0.61	0.70
		R_s (Ω)	37.55	60.58
Norde	***F(V)***	***ϕ_b (eV)***	0.72	0.75
		R_s (Ω)	86.75	121.62

R_s, n and ϕ_b values of the heterojunction can be determined using conventional J-V and Cheung-Cheung method [22]. Cheung-Cheung method has been defined by Eq. (10), Eq. (11) and Eq. (12) as described below:

$$\frac{dV}{d(lnJ)} = JR_s + n\left(\frac{kT}{q}\right) \quad (10)$$

$$H(J) = V - \left(\frac{nkT}{q}\right) ln\left(\frac{J}{AA^*T^2}\right) \quad (11)$$

$$H(J) = JR_s + n\phi_b \quad (12)$$

Fig. 7a shows dV/dln(J)-J characteristics of CIGS hetero-junction for darkness and illumination conditions. dV/dln(J)-J curves in Fig. 6 was determined from Eq. (10). The slope and the y-axis intercept in dV/dln(J)-J curves in Fig. 6a give R_s and nkT/q, respectively. The ideality factor and R_s values obtained from dV/dln(J)-J curve for darkness and illumination conditions have been given to be 6.57 and 32.72Ω; 3.86 and 52.00 Ω, respectively. H(J)-J curve in Fig. 7b have been determined from forward bias of log J-V characteristics in Fig. 5 and using Eq. (11). The slope and the y-axis intercept in H(J)-J curve show JR_s and $n\phi_b$ in Eq. (12), respectively. R_s and ϕ_b have been determined by H(J)-J curve in the darkness and illumination conditions have been determined to be 37.55Ω and 0.61 eV; 60.58Ω and 0.70 eV, respectively. The results for the barrier height calculated by Cheung-Cheung method have been found slightly different compared to the conventional J-V curve and Cheung-Cheung methods can be concluded that is based on the use of the reverse bias and forward bias region of the J-V and, respectively.

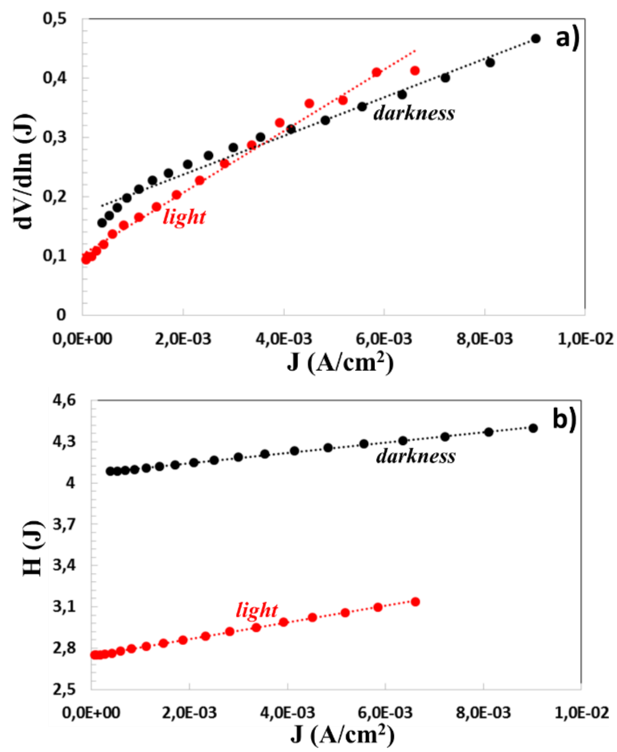

Fig. 7. **a)** dV/dln(J)-J and **b)** H(J)-J characteristics CIGS/n-Si hetero-junctions to darkness and illumination

Norde method was used to determine the serial resistivity and barrier height of the heterojunction [23]. Norde method is stated by Eq (13):

$$F(V,\gamma) = \frac{V}{\gamma} - \frac{kT}{q} ln\left(\frac{J(V)}{AA^*T^2}\right) \quad (13)$$

where γ is the first constant higher than ideality factor determined from log J-V curve. Also, R_s and ϕ_b values are calculated by Eq.(14) and Eq.(15) of Norde method;

$$\phi_b = F(V_o) + \frac{V_o}{\gamma} - \frac{kT}{q} \tag{14}$$

$$R_s = \frac{\gamma - n}{I_{min}} \frac{kT}{q} \tag{15}$$

where V_0 is a voltage that corresponds to the minimum $F(V_0)$ value of F(V)-V curve in Fig. 8. I_{min} is a current for the minimum voltage in J-V curve. R_s and ϕ_b values of the hetero-junction have been calculated to be 86.75Ω and 0.72 eV; 121.62Ω and 0.75 eV by Norde method to darkness and illumination conditions, respectively, and found to be higher than that calculated by other methods. This situation can be attributed that the calculation can be performed using Norde method calculations is based on the all forward bias region in J-V curve [24].

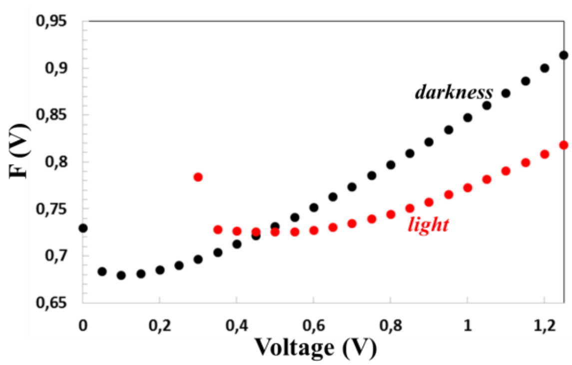

Fig. 7. F(V)-V curve of CIGS/n-Si heterojunction in the darkness and illumination

According to the J-V curve in Fig. 8, PV parameters of CIGS/n-Si solar cell can be determined to be J_{sc}=0.46 mA/cm^2, V_{oc}=300 mV, FF=0.14 and η= 0.024%. The defects, traps and hanging bonds in the interface, surface resistance of the thin film, contact resistances of Ag and Al metals can cause low J_{sc} and FF values. Because the ultra-thin film is so thin, pinholes and shunt paths can form in the thin film, which can generate leakage current. CIGS ultrathin film formed in small sized particles has multiple grain boundaries and photo-excited minority charge carriers which can recombine in traps and defects hidden within these boundaries. Also, the light falls directly on CIGS ultrathin film and since CIGS ultrathin film is in 420 nm thickness, the photo-excited minority charge carriers formed in CIGS undergo recombination on Ag contact before they reach the depletion region [6, 25, 26]. These negative factors can cause low J_{sc} and FF values and thus efficiency of CIGS/n-Si solar cell. However, CIGS solar cell based on Si exhibits PV properties. By adjusting CIGS ultrathin film to optimum thickness, and using contact metals with more ideal work functions, CIGS/Si heterojunction solar cells can be produced for the tandem solar cells with high performance.

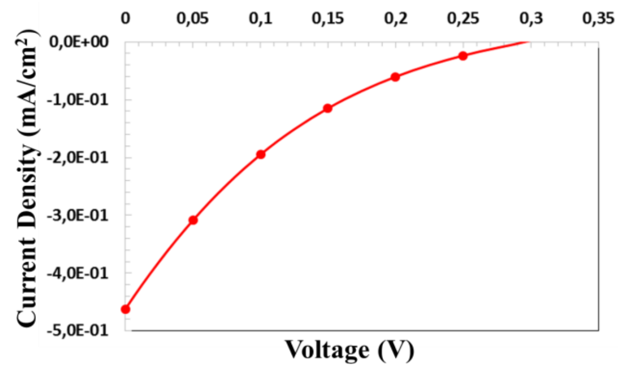

Fig. 8. J-V curve of CIGS/n-Si heterojunction solar cell

IV. Conclusion

In this study, we have grown CIGS ultrathin film in 420 nm thickness, using PLD system. CIGS ultrathin film has a single crystal structure and its crystal size, dislocation density and microstrain are 65.71 nm, 0.2 × 1015 (lines/m^2) and 0.55× 10^{-3}, respectively. CIGS ultrathin film is In-rich, in which Cu and (In+Ga) ratios are very close to each other and its band gap is 1.37 eV. RR value of CIGS heterojunction in the dark and illumination conditions are 2.22 and 0.24, respectively. CIGS heterojunction's n, ϕ_b, R_s values have been determined to be 2.90, 0.54 eV, 54.63 Ω and 3.71, 0.49 eV, 66.33 Ω from log J-V curve, for the darkness and illumination conditions, respectively. These electrical parameters have been calculated by Cheung-Cheung and Norde methods, and found as partially compatible with each other. CIGS/n-Si solar cell's photovoltaic parameters are J_{sc}=0.46 mA/cm2, V_{oc}=300 mV, FF=0.14 and η= 0.024%. The defects, traps and hanging bonds in the interface, pinholes, shunt paths, contact resistances, grain boundaries, the recombination on the contact can cause low J_{sc}, FF values and thus efficiency of CIGS/n-Si solar cell. However, CIGS/n-Si solar cell can be considered a preliminary study for CIGS tandem solar cells and many improvement studies should be done on this solar cell in this direction.

Acknowledgment

Authors kindly would like to thank,

- Selçuk University, High Technology Research and Application Center and
- Selçuk University, Laser Induced Proton Therapy Application and Research Center for supplying with Infrastructure and
- Selçuk University, Scientific Research Projects Coordination (BAP) Unit for grands via projects with references of 20401018 and 18401178

REFERENCES

[1] Bhatnagar, A., A. Johari, and V. Janyani. Performance analysis of thin film CIGS solar cell at different values of thickness, bandgap and temperature through numerical simulation. in Nanoengineering: Fabrication, Properties, Optics, Thin Films, and Devices XVII. 2020. International Society for Optics and Photonics.
https://doi.org/10.1117/12.2567882

[2] Powalla, M., et al., Advances in cost-efficient thin-film photovoltaics based on Cu (In, Ga) Se2. Engineering, 2017. 3(4): p. 445-451.
https://doi.org/10.1016/J.ENG.2017.04.015

[3] Song, N., et al., Epitaxial Cu2ZnSnS4 thin film on Si (111) 4 substrate. Applied Physics Letters, 2015. 106(25): p. 252102.
https://doi.org/10.1063/1.4922992

[4] Song, N., Epitaxial Growth of Cu2ZnSnS4 Thin Films forTandem Solar Cells. 2015.

[5] Gezgin, S.Y. and H.Ş. Kılıç, The electrical characteristics of ITO/CZTS/ZnO/Al and ITO/ZnO/CZTS/Al heterojunction diodes. Optik, 2019. 182: p. 356-371.
https://doi.org/10.1016/j.ijleo.2019.01.014

[6] Gezgin, S.Y., A. Houimi, and H.Ş. Kılıç, Production and photovoltaic characterisation of n-Si/p-CZTS heterojunction solar cells based on a CZTS ultrathin active layers. Optik, 2019. 199: p. 163370.
https://doi.org/10.1016/j.ijleo.2019.163370

[7] Oulmi, N., et al., CuIn 0.7 Ga 0.3 Se 2 thin films' properties grown by close-spaced vapor transport technique for second-generation solar cells. Materials for Renewable and Sustainable Energy, 2019. 8(3): p. 1-8.
https://doi.org/10.1007/s40243-019-0151-2

[8] Chen, S.-C., et al., Growth and characterization of Cu (In, Ga) Se 2 thin films by nanosecond and femtosecond pulsed laser deposition. Nanoscale research letters, 2014. 9(1): p. 1-7.
https://doi.org/10.1186/1556-276X-9-280

[9] Ghanbari, E., M. Zahedifar, and M. Moradi, Improving CIGS thin film by evaporation of CIGS nanoparticles without phase change. Applied Physics A, 2019. 125(5): p. 1-9.
https://doi.org/10.1007/s00339-019-2561-5

[10] Kalita, P.K., B. Sarma, and H. Das, Structural characterization of vacuum evaporated ZnSe thin films. Bulletin of Materials Science, 2000. 23(4): p. 313-317.
https://doi.org/10.1007/BF02720089

[11] Prabahar, S. and M. Dhanam, CdS thin films from two different chemical baths—structural and optical analysis. Journal of Crystal growth, 2005. 285(1-2): p. 41-48.
https://doi.org/10.1016/j.jcrysgro.2005.08.008

[12] Cohen, J.D., Identifying the Electronic Properties Relevant to Improving the Performance of High Band-Gap Copper Based I-III-VI2 Chalcopyrite Thin Film Photovoltaic Devices: Final Subcontract Report, 27 April 2004-15 September 2007. 2008, National Renewable Energy Lab.(NREL), Golden, CO (United States).
https://doi.org/10.2172/937345

[13] Farag, A., H. Soliman, and A. Atta, Analysis of dark and photovoltaic characteristics of Au/Pyronine G (Y)/p-Si/Al heterojunction. Synthetic metals, 2012. 161(23-24): p. 2759-2764.
https://doi.org/10.1016/j.synthmet.2011.10.017

[14] Makhlouf, M., M. El-Nahass, and M. Zeyada, Fabrication, temperature dependent current-voltage characteristics and photoresponse properties of Au/α-PbO2/p-Si/Al heterojunction photodiode. Materials Science in Semiconductor Processing, 2017. 58: p. 68-75.
https://doi.org/10.1016/j.mssp.2016.11.015

[15] Buscema, M., et al., Photocurrent generation with two-dimensional van der Waals semiconductors. Chemical Society Reviews, 2015. 44(11): p. 3691-3718.
https://doi.org/10.1039/C5CS00106D

[16] Tataroğlu, A., et al., Photoconducting properties of Cd 0.4 ZnO 0.6/p-Si photodiode by sol gel method. Journal of Electroceramics, 2014. 32(4): p. 369-375.
https://doi.org/10.1007/s10832-014-9920-6

[17] Ali, S.M., et al., Fabrication and SILAR cycle-dependent characterization of CdS/p-Si heterojunction photodetector. Journal of Materials Science: Materials in Electronics, 2020. 31(3): p. 2530-2536.
https://doi.org/10.1007/s10854-019-02789-6

[18] Balaji, M., J. Chandrasekaran, and M. Raja, Characterization of WMoO3 thin films and its n-WMoO3/p-Si junction diodes via JNS pyrolysis technique. Zeitschrift für Physikalische Chemie, 2017. 231(5): p. 1017-1037.
https://doi.org/10.1515/zpch-2016-0861

[19] Roy, S., et al., A tetranuclear nickel/lead complex with a salen type Schiff base: synthesis, structure and exploration of photosensitive Schottky barrier diode behaviour. New Journal of Chemistry, 2019. 43(13): p. 5020-5031.
https://doi.org/10.1039/C8NJ05616A

[20] Özerli, H., et al., Electrical and photovoltaic properties of Ag/p-Si structure with GO doped NiO interlayer in dark and under light illumination. Journal of Alloys and Compounds, 2017. 718: p. 75-84.
https://doi.org/10.1016/j.jallcom.2017.05.121

[21] Ashery, A., M.M. Elnasharty, and I. El Radaf, Fabrication and electrical characterization of the Al/n-Si/CZTSe4/Ag heterojunction. Physica B: Condensed Matter, 2021. 609: p. 412707.
https://doi.org/10.1016/j.physb.2020.412707

[22] Cheung, S. and N. Cheung, Extraction of Schottky diode parameters from forward current-voltage characteristics. Applied physics letters, 1986. 49(2): p. 85-87.
https://doi.org/10.1063/1.97359

[23] Norde, H., A modified forward I-V plot for Schottky diodes with high series resistance. Journal of applied physics, 1979. 50(7): p. 5052-5053.
https://doi.org/10.1063/1.325607

[24] Basman, N., Effect of a new methacrylic monomer on diode parameters of Ag/p-Si Schottky contact. Informacije MIDEM, 2016. 46(4): p. 190-196.

[25] Gezgin, S.Y., et al., The Effect of CZTS Ultrathin Film Thickness on the Electrical Characteristic of CZTS/Si Heterojunction Solar Cells in the Darkness and under the Illumination Conditions. Silicon, 2020: p. 1-13.
https://doi.org/10.1007/s12633-020-00847-x

[26] Gezgin, S.Y.ğ.t. and H.Ş. Kılıç, An improvement on the conversion efficiency of Si/CZTS solar cells by LSPR effect of embedded plasmonic Au nanoparticles. Optical Materials, 2020. 101: p. 109760
https://doi.org/10.1016/j.optmat.2020.109760

Associate Professor. Dr. Serap YİGİT GEZGİN graduated from Süleyman Demirel University, Faculty of Science, Department of Physics, in 2002. In 2009, She completed her master studies in Department of Physics, High Energy and Plasma Physics at Süleyman Demirel University. She comleted her doctor of philosophy in the Department of Physics and Atomic and Molecular Physics at Selcuk University, in 2019. He was appointed Associate Professor in 2021, and still continues to work as an Instructor at Selçuk University, Faculty of Science.

Associate Professor. Dr. Yasemin GÜNDOĞDU graduated from Selcuk University, Faculty of Science, Department of Physics, in 2011. In 2014, She completed her master studies in Department of Physics, Atomic and Molecular Physics at Selcuk University. She comleted her doctor of philosophy in the Department of Physics and Atomic and Molecular Physics at Selcuk University, in 2018. He was appointed Associate Professor in 2019, and still continues to work as an Instructor at Selçuk University, Faculty of Science.

Prof.Dr. Hamdi Sukur Kılıç graduated from Selcuk University, Faculty of Engineering and Architecture, Department of Physics Engineering, Physics Engineer in 1988. In 1990, he started to work as a research assistant in the Department of Physics and Atomic and Molecular Physics at Selçuk University. He completed his doctoral studies at Glasgow University in 1997. He was appointed Assistant Professor in 1998, Associate Professor in 2002 and Professor in 2007, and still continues to work as an Instructor at Selçuk University, Faculty of Science.